

Red Phosphorus–Controlled Decomposition for Fire Retardant PA 66

B. SCHARTEL, R. KUNZE, D. NEUBERT

Federal Institute for Materials Research and Testing, Unter den Eichen 87, 12205 Berlin, Germany

Received 3 April 2001; accepted 11 June 2001

ABSTRACT: The thermal degradation and the combustion behavior of glass fiber–reinforced PA 66 materials containing red phosphorus were investigated. Thermogravimetry (TG), TG coupled with FTIR, and TG coupled with mass spectroscopy were used to investigate the thermal decomposition. The flame retardant red phosphorus was investigated with respect to the decomposition kinetics and the release of volatile products. The combustion behavior was characterized using a cone calorimeter. Fire risks and fire hazards were monitored versus external heat fluxes between 30 and 75 kW/m². Red phosphorus acts in the solid phase and its efficiency depends on the external heat flux. The use of red phosphorus results in an increased amount of residue and in a corresponding decrease in total heat release. The decrease of the mass loss rate peak results in a corresponding decrease of the peak heat release. With increasing external heat flux applied the first effect on the total heat release decreases linearly, whereas the second effect on the peak heat release expands linearly. The investigation provides insight into the mechanisms of how the fire retardant PA 66 is achieved by red phosphorus controlling the degradation kinetics. Taking into account that a decrease of the volatile products also leads to a decrease of heat production in the flame zone and that the char acts as heat transfer barrier, a reduced pyrolysis temperature is suggested as a further feedback effect. © 2002 John Wiley & Sons, Inc. *J Appl Polym Sci* 83: 2060–2071, 2002

Key words: PA 66; red phosphorus; fire retardancy; TG-FTIR; cone calorimeter

INTRODUCTION

Phosphorous-containing compounds including red phosphorus, inorganic phosphates, organophosphorus compounds, and so forth have been discussed as promising flame retardants for decades. Recently, the discussion on toxicological effects for halogenated fire retardants and the resulting legislative restrictions have fostered

the development of phosphorous-containing compounds as alternative halogen-free flame-retardant additives. Because they function predominantly in the condensed phase, promoting char formation, they are promising additives to reduce fire risk and fire hazards such as the production of optical-dense and corrosive smoke. Even though elemental phosphorus has a reputation for being highly flammable, the amorphous form, red phosphorus, was found to be an effective flame retardant additive¹ in a wide range of polymer materials.² One well-known example is glass-filled PA 66 containing only 6–8% red phosphorus, reaching V-0 classifications in the UL-94 test.³ Such flame retar-

Correspondence to: B. ScharTEL (bernhard.schartel@bam.de).

Contract grant sponsor: BASF AG (Germany).

Journal of Applied Polymer Science, Vol. 83, 2060–2071 (2002)
© 2002 John Wiley & Sons, Inc.
DOI 10.1002/app.10144

dant PAs are sold successfully as commercial products mainly for use in electric and electronic applications.

Despite their commercial use, the scientific understanding of the thermal and the fire behavior is the object of extensive research activities, thus leading to a large number of recent publications in this field.^{4–6} Most sources tend to describe the differences in the thermal decomposition or the combustion behavior and judge the effectiveness of distinct phosphorus-containing flame retardants. In contrast to these studies, it is the intention of the work presented here to figure out how phosphorus-controlled degradation of PA 66 influences the combustion behavior. Therefore, the thermal degradation of different glass fiber-reinforced PA 66 materials was investigated by thermogravimetry (TG), TG coupled with FTIR (TG-FTIR), and TG coupled with mass spectroscopy (TG-MS). Their combustion behavior was characterized with a cone calorimeter (CC). The fire risks (time to ignition, heat release rate, total heat release) as well as the fire hazards (smoke release rate, total smoke release, CO production) were monitored versus heat fluxes between 30 and 75 kW/m². The wide range of external heat fluxes makes the conclusions drawn from this study valuable for different realistic fire scenarios and fire tests. The thermal degradation and the resulting products were characterized by TG-MS and TG-FTIR. TG investigations with varying heating rates enable a detailed description of the kinetics involved and permit a quantitative evaluation of the combustion behavior.

EXPERIMENTAL

Samples

Seven glass-filled PA 66 materials (Ultramid® [BASF AG, Ludwigshafen, Germany]) were investigated: A3EG5 (PA66-GF25, UL 94 HB; density $\rho = 1.32 \text{ g/cm}^3$; thermal conductivity $k = 0.34 \text{ W m}^{-1} \text{ K}^{-1}$; specific heat $c = 1.6 \text{ J g}^{-1} \text{ K}^{-1}$), A3EG7 (PA66-GF35, UL 94 HB; $\rho = 1.41 \text{ g/cm}^3$; $k = 0.35 \text{ W m}^{-1} \text{ K}^{-1}$; $c = 1.5 \text{ J g}^{-1} \text{ K}^{-1}$), A3X3G5 (PA66-GF25 FR, UL 94 V-1; $\rho = 1.34 \text{ g/cm}^3$; $k = 0.33 \text{ W m}^{-1} \text{ K}^{-1}$; $c = 1.5 \text{ J g}^{-1} \text{ K}^{-1}$), A3X3G7 (PA66-GF35 FR, UL 94 V-1; $\rho = 1.45 \text{ g/cm}^3$; $k = 0.34 \text{ W m}^{-1} \text{ K}^{-1}$; $c = 1.4 \text{ J g}^{-1} \text{ K}^{-1}$), A3X2G5 (PA66-GF25 FR, UL 94 V-0; $\rho = 1.34 \text{ g/cm}^3$; $k = 0.33 \text{ W m}^{-1} \text{ K}^{-1}$; $c = 1.5 \text{ J g}^{-1} \text{ K}^{-1}$), A3X2G7 (PA66-GF35 FR, UL 94 V-0; $\rho = 1.45 \text{ g/cm}^3$; $k = 0.34 \text{ W m}^{-1} \text{ K}^{-1}$; $c = 1.4$

$\text{J g}^{-1} \text{ K}^{-1}$), A3XZG5 (PA66-GF25 FR, UL 94 V-0; $\rho = 1.32 \text{ g/cm}^3$; $k = 0.33 \text{ W m}^{-1} \text{ K}^{-1}$). X (FR) marks the products with red phosphorus as fire retardant additive. G5 (GF25) and G7 (GF35) mark the glass fiber content. The materials were provided by BASF AG in plate (10 × 10 cm, 2.8 mm thick) and granulate form. The plates were used for the cone calorimeter investigations, whereas the granulate was used in the thermogravimetric experiments. The samples without red phosphorus are milky white and the samples with red phosphorus are reddish brown.

Thermogravimetry (TG) Evaluation of Decomposition Kinetics

The thermogravimetry experiments were carried out on 15-mg samples with a TGA/SDTA 851 (Mettler/Toledo, Gießen, Germany) instrument under nitrogen. Heating rates of 2, 5, 10, and 20 K/min were applied. The degradation kinetics were evaluated using the Mettler/Toledo software for model-free kinetics.

TG Coupled with Mass Spectroscopy (TG-MS)

The TG-MS analysis system consisted of a TG/DTA 220 (Seiko, Thermo Haake, Karlsruhe, Germany) coupled with a QMG 421 C quadrupole mass spectrometer (Balzer, Lichtenstein). A quartz capillary system was used to reduce the pressure from ambient to high vacuum, to permit the simultaneous recording of the mass spectra.⁷ Experiments were performed in the temperature range of 303–973 K under nitrogen and air at a flow rate of 200 mL/min. The applied heating rate was 10 K/min and the quartz capillary line was maintained at a temperature of 473 K. The sample mass was 10 mg. The characteristic fragments were determined by bar-graph measurements and were monitored versus the temperature in the multiple ion detection mode.

TG Coupled with Fourier Transform Infrared Spectroscopy (TG-FTIR)

A TGA/SDTA 851 (Mettler/Toledo) coupled with an FTIR-Spectrometer Nexus 470 (Nicolet Instruments, Offenbach, Germany) was used. The measurements were performed in the temperature range of 298–873 K with a heating rate of 5 K/min and a nitrogen flow of 30 mL/min. The mass of the samples was 15 mg. The coupling capillary system was heated to 473 K and the gas sample cell of the FTIR spectrometer to 483 K.

Table I Thermogravimetric Analysis Results

Sample	Glass Fiber Content (%)	Residue (%)	DTG-Peak (K) (DTG-Shoulder [K])	Maximum Rate (%/K)
A3EG5	25	27	675 ^a (~ 718)	1.35
A3EG7	35	36	679 ^a (~ 718)	1.09
A3X2G5	25	29	684 ^b (~ 718)	0.69
A3X2G7	35	38	639; 723 ^c	0.59

^a The flank of the peaks indicates further processes between 645 and 660 K.

^b The flank of the peaks indicates further processes around 623 and 660 K.

^c The flank of the peaks indicates further processes around 695 and 615 K.

After every measurement the sample cell was cleaned with a 1373 K hot oxygen stream to minimize condensation.

Cone Calorimeter (CC)

The combustion behavior was characterized by a cone calorimeter according to ASTM E 1354/ISO 5660 (Fire Testing Technology, East Grinstead, UK). Distinct external heat fluxes (30, 40, 50, 60, 75 kW/m²) were applied. The experiment was stopped when no further significant mass loss was observed. The volatile products were ignited by spark ignition or with a small flame, respectively. The samples matched the thickness of interest for applications, but they were thin with respect to the sample geometry recommended by the standards. The fire-retardant systems showed an intumescent behavior, decreasing the distance to the cone heater. All the samples were measured using a retainer frame, to reduce unrepresentative edge burning in the horizontal position. The calculations were performed using 0.008836 m² instead of 0.01 m², taking into account the decreased sample area.⁸ The material protected by the frame was only partially combusted for higher heat fluxes; the influence on the results, which are of minor importance, can be neglected. The experiments are based on the standard but are, strictly speaking, not exactly according to it. However, the results presented are consistent and reproducible.

RESULTS AND DISCUSSION

Thermal Decomposition: Mass Loss and Products for a Constant Heating Rate

The TG results are summarized in Table I and Figure 1 for samples A3EG5, A3X2G5, A3EG7,

and A3X2G7 under nitrogen using a heating rate of 10 K/min. Comparison of the TG and DTG data for the different materials leads to the conclusion that all samples show a decomposition characterized by a second step following the main decomposition step. This is represented by a shoulder or maximum, respectively, indicated at 720 K in the DTG data for all samples. The DTG data indicate at least one further process at the low-temperature flank of the main decomposition process. The investigation of the release rate for the different products that is described later in this article confirms such a complex structure. The temperature interval typical for the decomposition is between 625 and 739 K for the samples without red phosphorus and between 583 and 753 K for the samples with red phosphorus. For samples without red phosphorus the overlap of the decomposition steps at heating rates above 10 K/min is so distinct, that the second step forms a shoulder only in the TG curves. The results presented here correspond to the data published for PA 66 samples.^{9,10} By adding red phosphorus as a fire-retar-

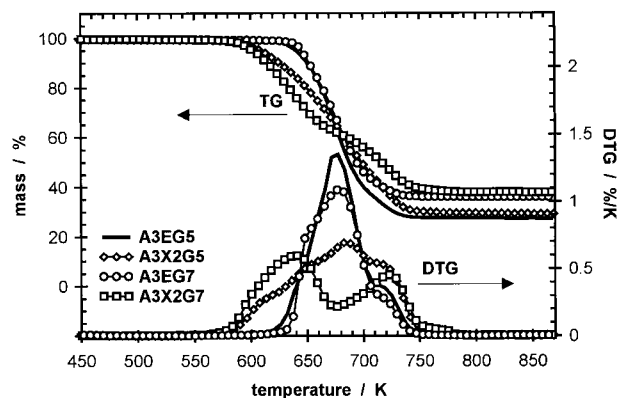


Figure 1 TG and DTG under nitrogen (heating rate 10 K/min).

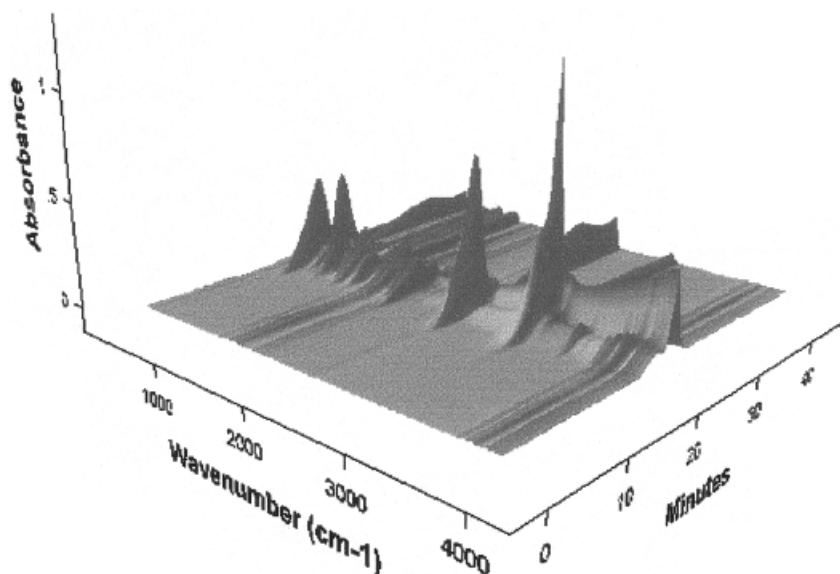


Figure 2 FTIR results during a TG-FTIR experiment.

dant additive, the two main processes become clearly separated. The onset temperature of decomposition is decreased by about 40 K, whereas the end-set temperature is increased about 15 K. This broadening of the whole decomposition region results in a decrease of the DTG values by a factor of 2. The residue for high temperatures (>750 K) mainly represents the glass-fiber content. The samples with red phosphorus show an additional residue at such high temperatures in the region of a few mass percent. This small increase may indicate remaining phosphorus rather than the formation of a stable char.

With TG-FTIR or TG-MS an interpretation of the decomposition in terms of the pyrolysis gases is possible. The interpretation of the FTIR spectra can be difficult, given that a superposition of the various signals is caused by the various gases. In the case of TG-MS the detected masses are often ambiguous in terms of possible corresponding fragments. By using both methods we have reached unambiguous interpretations of the data obtained without using further assumptions on the material or the active decomposition pathway.

The main pyrolysis products are carbon dioxide (CO_2), cyclopentanone ($\text{C}_5\text{H}_8\text{O}$), water (H_2O), and ammonia (NH_3). Furthermore, hydrocarbons and amines were found. The results are in good correspondence to comparable published studies.^{11–14} Figure 2 displays the FTIR data versus the time of a TG-FTIR investigation. The time

axis also indicates the temperature because we used a constant heating rate during the experiment. By using the spectra of the distinct experimental times (e.g., the maxima of the mass loss), the pyrolysis products can be identified. By following a product-specific characteristic of the spectrum versus the time, a chemigram could be evaluated that displays the changes of the product release. Such chemigrams are given in Figure 3 for A3EG7 and A3X2G7, displaying the characteristic release of CO_2 , $\text{C}_5\text{H}_8\text{O}$, NH_3 , and hydrocarbons. Corresponding evaluations of the MS results were performed by determining the ion current for a typical fragment versus the time or temperature, respectively. The results from the

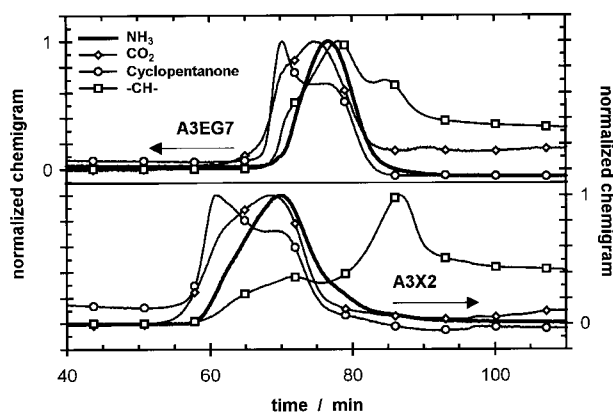


Figure 3 Chemigrams of CO_2 , $\text{C}_5\text{H}_8\text{O}$, NH_3 , and hydrocarbons for A3EG7 and A3X2G7.

TG-FTIR and the TG-MS investigations correlate well with each other and also with the DTG data. The overall picture obtained from the evaluation of the results from the different techniques is consistent.

The detected decomposition products are the same for all the samples without and with red phosphorus. In the main decomposition step NH_3 , CO_2 , H_2O , and cyclopentanone were found. The decomposition step following the main step is characterized by hydrocarbons and amines. The minor structure assumed for the increasing temperature flank of the main decomposition could be confirmed by the corresponding data of the pyrolysis products CO_2 , cyclopentanone, and water but not for NH_3 . NH_3 corresponds only to the main peak. The main difference between the samples without and with red phosphorus is given by the temperature shift of the main decomposition step.

The presence of HCN and PH_3 as possible fire hazards was investigated. The FTIR spectra do not provide evidence that would indicate the production of such secondary products. This was confirmed by mass spectroscopy investigations, which are more sensitive. Even with the most sensitive resolution (10^{-13} A) for the ion current no trace of PH_3 ($m/e = 34$) could be found. The typical mass for HCN ($m/e = 27$) was found in the mass spectra but has to be interpreted as the common fragment C_2H_3 ($m/e = 27$), given that it occurs parallel to fragments with the masses 39, 41, 42, and 56 that clearly indicate a series C_xH_y .

Thermal Decomposition: Kinetics

For A3EG5 and A3X2G5 the kinetics of decomposition were investigated by varying the heating rates in the TG experiment. For low heating rates the two main steps of decomposition can be distinguished for both samples with and without red phosphorus. The data evaluation was based on the isoconversion method and therefore it requires a model-free kinetics data evaluation.¹⁵⁻¹⁷ The processes are thermally activated and can be described with an Arrhenius equation. The activation energy is constant only for a certain conversion. A model for the reaction is not required but is assumed to be unchanging for a certain conversion. Such a data evaluation is applicable to both simple and complex processes, delivers reliable results with low relative errors, and does not bear the ambiguity peculiar to alternative methods. It is obvious that the decomposition here is complex, at least in the sense of a compet-

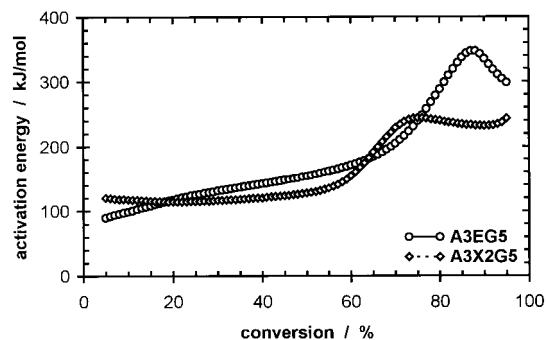


Figure 4 Activation energy dependent on the conversion.

itive multistep reaction, suggesting such a model-free data evaluation is most suitable. The obtained results for the activation energy are given versus the conversion in Figure 4 for A3EG5 and A3X2G5. The qualitative behavior of the activation energy versus the degree of decomposition is similar for both samples. It can be differentiated in two regions, confirming that two subsequent processes are dominant. This behavior corresponds to the two main subsequent processes concluded for the DTG data. Up to a 60% degree of decomposition, sample A3EG5 shows a moderate increase of the activation energy from 95 to 165 kJ/mol. Beyond a 60% degree of composition the activation energy increases sharply up to a value of approximately 320 kJ/mol. The activation energy was not found to be constant for any range of conversion. Hence, an overlap of different processes can be concluded for the whole range of conversion. For sample A3X2G5 the two regions are more clearly separated than they are for A3EG5. This difference corresponds to the separation of the two processes observed in the DTG data for red phosphorus-containing samples. The activation energy (119 kJ/mol) is nearly constant in the region between 0 and 60% conversion. The constant activation energy is characteristic for one active process. Beyond 60% conversion it increases to a value of approximately 230 kJ/mol. It becomes clear that the red phosphorus results in a decrease of the activation energy, especially for high degrees of decomposition. The results are in good correspondence with comparable results in the literature.^{9,18} An increase of the activation energy (130–225 kJ/mol) was reported in dependence on the decomposition for PA 66 and a two-step process was found for phosphorus-containing fire-retardant compounds, that is, PA 66 with ammonium polyphosphate. The latter system was

characterized by decreased activation energies to 120 and 165 kJ/mol. The change of the behavior upon reaching a decomposition of 60% was assumed to indicate that a radical process would become increasingly important.

Taking into account the results for DTG and the release of the distinct products, two main processes are identified. The first process leads to the production of NH_3 , CO_2 , H_2O , and cyclopentanone and is characterized by an activation energy around 120 kJ/mol. The second process is characterized by production of hydrocarbons and amines and by higher activation energies.

Combustion Behavior: Visual Observation

At the beginning of the cone calorimeter experiments, a black skin was observed for both kinds of materials. This is ascribed to thermooxidative decomposition reactions that take place on the surface of the sample before ignition. Such a decomposition under air was previously described for TG experiments on nylon.⁵ It is characterized by the production of a more stable char in comparison to decomposition under nitrogen. The subsequently observed bubbling under this skin can be interpreted as anaerobic decomposition because the skin does not increase in thickness. After ignition, the polymeric materials burn homogeneously with a stable flame zone above the surface. The polymer decomposition is assumed to occur in the absence of oxygen apart from the described effect at the beginning of the experiments. The samples without red phosphorus combust almost completely. A brittle, glassy white glass-fiber framework remains after the combustion. It is widened during the combustion so that the thickness of the samples increases by a factor of 1.2–2. For the samples with red phosphorus an intumescent behavior is observed. A black residue is obtained and the sample thickness increases by a factor of 4–5.3 for samples A3X2G5, A3X2G7, A3X3G7, and A3X3G7 and by a factor of 1.35–4.6 for sample A3XZG5. With increasing external heat fluxes, the remaining material becomes brittle. The residues indicate that their difference from that of a glass-fiber framework vanishes for increasing heat fluxes, even though the different color still proves a residue beyond the glass fibers. This qualitative interpretation is discussed quantitatively in terms of the total mass loss in the following section. However, apart from the remaining skin for these materials, all samples look quite homogeneous after burning. It can be con-

cluded that the pyrolysis zone moved through the complete sample in all experiments.

Combustion Behavior: Fire Risks

In Table II the fire risks are summarized in terms of the time to ignition, the total heat release, and peaks of the heat release rate. The obtained data for the time to ignition are according to eq. (1), which is considered suitable to describe the dependency of the time to ignition on the external heat flux.^{19,20} The data and the fits using eq. (1) are plotted in Figure 5 and correlate well with each other.

$$t_{ig}^{1/2} = \left[\frac{\epsilon}{\sqrt{\frac{2}{3}} k \rho c (T_{ig} - T_0)} \right] \dot{q}_{ext}'' - \left[\frac{h_c (T_{ig} - T_0) + \epsilon \sigma T_{ig}^4}{\sqrt{\frac{2}{3}} k \rho c (T_{ig} - T_0)} \right] \quad (1)$$

where t_{ig} is the time to ignition; T_{ig} is the ignition temperature; h_c is the convective heat transfer coefficient; T_0 is the temperature for $t = 0$; σ is the Stefan–Boltzmann constant; k is the thermal conductivity; ρ is the density; ϵ is the emissivity; c is the specific heat; and \dot{q}_{ext}'' is the external heat flow per unit time per unit area.

Based on the data fits, ignition temperatures can be calculated using eq. (1), assuming an emissivity of $\epsilon = 1$ for all samples. They were calculated to values between 740 and 820 K. Decreased times to ignition were determined for samples containing red phosphorus for low external heat fluxes. This is consistent with the described behavior of the decomposition onset in the TG experiments. However, the times to ignition do not vary significantly. Furthermore, the difference between the times to ignition vanishes for high external heat fluxes.

The maximum heat release rate and the total heat release are both important to determine the fire risks. The peak heat release rate influences the flame spread. The total heat release contributes to the total heat release in a fire. The heat release rate was found to correspond with the mass loss rate and the total heat release with the total mass loss. These relationships correspond to the TG experiments, proving that no significant change occurs in the kind of pyrolysis products. Again, we found that red phosphorus acts in the solid phase rather than in the gas phase. Just

Table II CC Results Versus the External Heat Flux for the Distinct Samples

Sample	Heat Flux (kW/m ²)	Time to Ignition (s [± 2 s])	Residue/ (% Mass [$\pm 1\%$])	Total Heat Release (MJ/m ² [± 5 MJ/m ²])	Peak of Heat Release Rate		Total Smoke Released (± 50)	CO Yield—6-min Average (kg/kg [± 0.003 kg/kg])
					(kW/m ² [± 10 kW/m ²])	(s [± 5 s])		
A3EG5	30	110	30.8	81.3	354	300	800	0.0134
	40	74	26.9	84.7	383	134	733	0.0130
	50	42	26	83.6	520	122	697	0.0125
	60	30	24.3	89.6	619	98	680	0.0120
	75	19	25.1	88.8	721	86	745	0.0138
A3X3G5	30	92	57.8	12.8	59	234	1136	[0.0831]
	40	65	43.8	54.3	133	117	1569	0.118
	50	39	39.3	62.8	222	63	1361	0.1358
	60	27	32.1	74	269	53	1770	0.1402
	75	18	28.7	75.3	303	45	1965	0.1267
A3X2G5	30	89	53.2	52.2	192	120	1304	0.1396
	40	62	47.3	66.6	213	83	1473	0.1411
	50	37	40.1	64.0	237	63	1712	0.1471
	60	28	33.1	77.4	280	57	1997	0.1463
	75	18	28.7	80.7	320	42	2189	0.1314
A3XZG5	30	101	49.9	48.4	158	138	1438	0.1631
	40	70	41.7	59.1	209	92	1722	0.1678
	50	41	38.7	64.2	237	77	1848	0.1685
	60	31	29.4	70.5	267	54	2170	0.1713
	75	19	27.8	80.3	310	54	2288	0.1301
A3EG7	30	113	40.6	79	372	276	586	0.0202
	40	71	38.8	77.1	364	186	710	0.0169
	50	43	35.9	73.7	472	128	790	0.0141
	60	31	34.4	83.2	552	92	700	0.0137
	75	21	34.2	80.3	647	77	835	0.0150
A3X3G7	30	117	65.6	25.2	101	144	888	0.0985
	40	68	55	51	167	84	1137	0.1177
	50	43	50.8	56.2	194	66	1152	0.1280
	60	31	44	63.3	221	53	1535	0.1426
	75	20	40.1	57.4	249	39	1670	0.1284
A3X2G7	30	98	66.4	29.2	127	123	761	0.0921
	40	66	58.3	42.7	176	84	1002	0.1188
	50	41	50.5	56.8	187	62	1233	0.1313
	60	30	45.8	61.2	225	48	1479	0.1392
	75	20	40.6	62	236	44	1701	0.1285

The fire risks (time to ignition, total heat release, and the peak of the heat release rate) and the fire hazards (total smoke release, CO production) are illustrated in comparison to the residue mass. All the displayed values are average values based on duplicate measurements.

after ignition, no difference was observed in the increase of the heat release rate for both types of samples. After an effective char layer is built up for the flame-retardant materials, the heat release rate differs significantly. An example for this behavior of the heat release rate and the corresponding total heat release is given in Figure 6 for samples without and with red phospho-

rus at the same external heat flux. For each material the results of two tests are shown, to demonstrate the good reproducibility. Just after the ignition the heat release rate curves are similar for both materials for a time period of 20 s before the red phosphorus-containing material displays a maximum heat release rate far below the maximum values for the materials without fire retar-

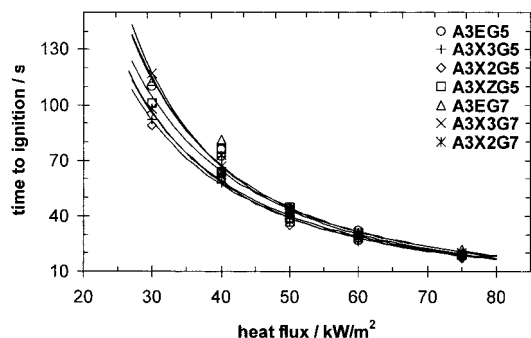


Figure 5 Time to ignition and corresponding fits using eq. (1) versus external heat flux.

dancy. Obviously, this maximum for the sample with red phosphorus is reached in a shorter time interval. We conclude that the heat barrier properties of the char at the top of the sample result in a decrease of the pyrolysis temperature. Furthermore, the barrier properties for volatiles and the decreased pyrolysis temperature restrict the mass transfer to the flame zone. This decreased mass transfer results in a reduced amount of heat production in the flame zone and therefore to a decreased feedback to the sample, which can be interpreted as a self-reinforcing fire-retardancy mechanism.

According to the TG experiments the temperature interval for the occurrence of a stable char is broadened, compared to that of the pure polymer, rather than its stability for high temperatures to be improved. Furthermore, a decreased pyrolysis temperature does not conclusively result in a re-

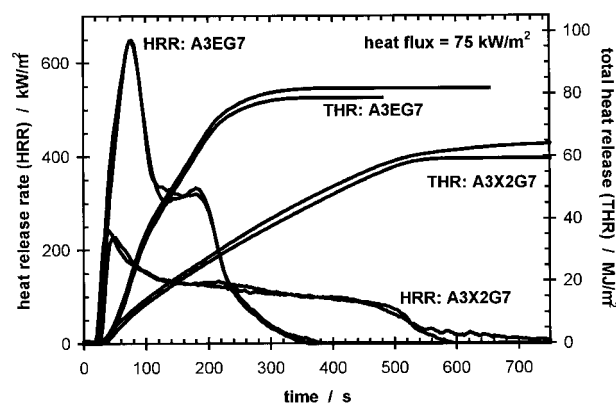


Figure 6 Heat release rate and total heat release for a system without (A3EG7) and with (A3X2G7) red phosphorus versus the time for an external heat flux of 75 kW/m^2 . For each material the results of two samples are shown.

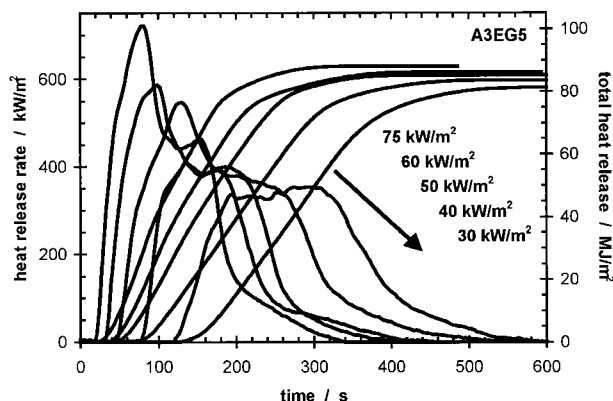


Figure 7 Heat release rate and total heat release for A3EG5 by varying the external heat flux.

duction of the total heat release. Thus it is not surprising that the time to flame out is found to be significantly increased, whereas the time to ignition is approximately equal. Hence, the time period in which the samples show a significant mass loss and a corresponding heat release is increased. Consequently, there are two time ranges in which the fire-retardant materials display a higher heat release than that of the A3E materials: first, before the generation of a protecting char layer, especially if the external heat flux is low and the ignition occurs significantly earlier; second, in the time interval between the flame out of the samples without and the flame out of the samples with fire retardant. This observation is not unusual for fire-retardant polymers, given that the peak of the heat release rate and the total heat release can be improved, even though the burning time period is increased or the ignition time is decreased.

A deeper insight into the effectiveness of the fire retardancy is achieved by varying the external heat fluxes. Additionally, the practical importance should be noted because different fire tests and fire scenarios correspond to different external heat fluxes. Figure 7 displays the rate of heat release and the total heat release for A3EG5, which is employed as an example for the materials without red phosphorus. Figure 8 displays how the external heat flux influences the rate of mass loss and the remaining mass for A3X2G5 as an example for samples with red phosphorus. The heat release rate corresponds to the mass loss rate and the total heat release corresponds to the total mass loss. As already discussed, the time to ignition increases with decreasing external heat flux. Also, the decreased external heat flux results

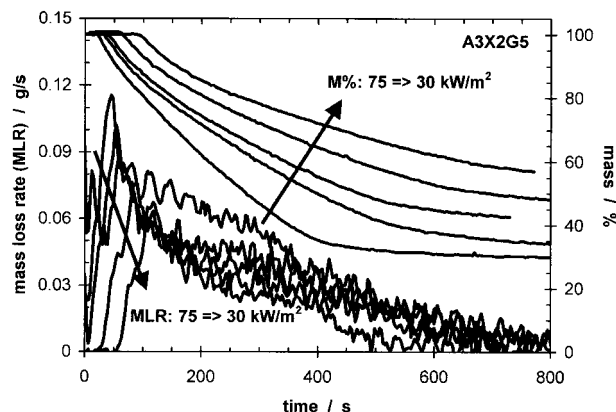


Figure 8 Mass loss rate and mass loss for A3X2G5 by varying the external heat flux.

in a decreased mass loss rate and a decrease of the total mass loss. For samples without red phosphorus the latter effect is clearly not as significant as the effect on the mass loss rate, in that the burning time is increased at a high level of mass loss rate. The samples containing red phosphorus are characterized by a large influence on the total mass loss and a less significant change of the peak heat release rate compared to that of the samples without red phosphorus.

In Figure 9 an overview of the results for the peak heat release versus the external heat flux is given for all investigated samples. The value of the heat release peaks increases linearly with increasing external heat flux. The increase in slope is clearly different for materials without and with red phosphorus. The relative effectiveness of the fire retardant red phosphorus increases for high external heat fluxes in terms of the maximum rate of heat release. This is most likely attributable to the fact that the mechanistic origin for the peak is changed from a noncharring

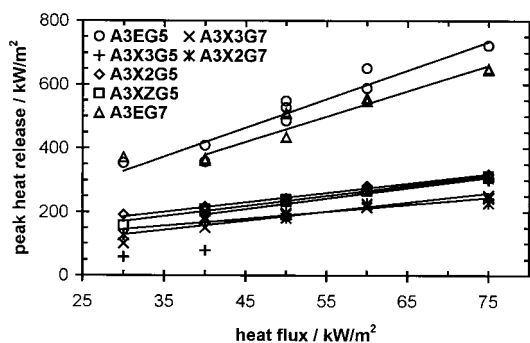


Figure 9 Heat release rate maxima versus the external heat flux.

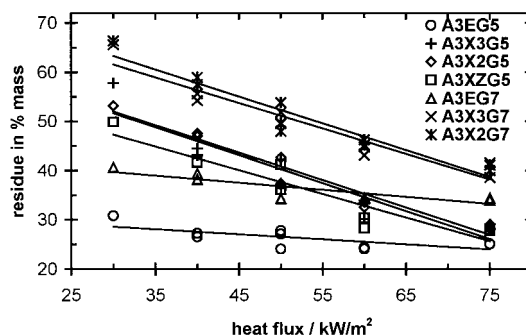


Figure 10 Residue versus the external heat flux.

to charring material, as discussed previously. The peak heat release is determined by the heat flux affecting the sample. This heat flux is established by adding the contributions of the external heat flux and the thermal feedback of the flame zone. The feedback of the flame zone depends on the rate of volatile products feeding the flame. This rate is increased for increasing heat flux resulting from the enhanced mass loss rate. Important limiting influences are the thermal conductivity of the sample and the diffusion rates of the products feeding the oxidation in the flame. Both are restricted for char-forming systems. It becomes clear that noncharring systems are characterized by a stronger increase of the peak heat release for increasing external heat flux compared to that of charring systems.

The mass losses and therefore the total heat releases of the materials without the fire-retardant additive increase slightly with increasing external heat fluxes. Figures 10 and 11, respectively, give an overview of the residues and total heat release versus the external heat flux for all investigated samples. The values of the total heat release just after the flame out was used for a

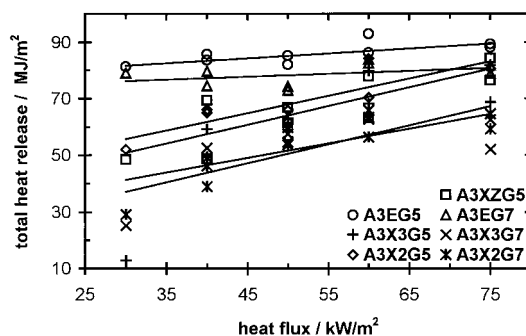


Figure 11 Total heat release versus the external heat flux.

systematic comparison. The residue at the end of the measurement was calculated as a percentage of the starting mass. The residues of the A3E materials are determined by the remaining glass-fiber content, which for the G7 materials is about 10% higher than that for G5 materials. In a first approximation, the change of the glass-fiber content from G5 to G7 has no influence on all the investigated properties, except that there is less combustible polymeric material in the samples. Therefore the results of corresponding samples differ by a constant value, which can be clearly seen in Figures 9, 10, and 11 for the peak heat release, the residue, and the total heat release, respectively. The external heat flux exerts only a minor influence on the residue for the polymers without red phosphorus, whereas the fire retardant samples show a large linear increase of residue from 5 to 20% in addition to the glass-fiber content for decreasing external heat fluxes from 75 to 30 kW/m².

This result is consistent with the qualitative description of the remaining materials described earlier. The total heat release is decreased for low external heat fluxes and levels off for high external heat fluxes compared to that of materials without red phosphorus. The relative effectiveness of the fire retardant red phosphorus increases for low external heat fluxes in terms of the total heat release. Therefore, the change of relative effectiveness versus the external heat flux is contrary for the total heat release compared with the maximum rate of heat release. It is particularly notable that the investigated system shows such a differentiation between peak heat release and total heat release. Therefore it becomes obvious that the concept of fire retardancy by char-forming systems works here by two mechanisms. On the one hand, the char acts as a barrier layer, influencing the mass and heat transfer, thus resulting in a decrease of the heat release rate. On the other hand, the char-forming process can lead to an increase of the thermally stable residue and consequently to a decrease of the total heat release resulting from a decrease of the total amount of combustible volatile products. It should be noted that for both mechanisms the occurrence of the other mechanism is not necessary.

The result that the fire-retardant effect diminishes for high external heat fluxes in terms of total mass loss and total heat release demands a further explanation. The burning for all of the samples results in homogeneous residues after

combustion. Hence, the formation of a thermally stable char should increase the residue by a certain amount that is nearly independent of the heat flux applied. A residue after a decomposition process, which is not stable at the pyrolysis temperature, should not influence the total mass loss and total heat release. As already discussed, the residue built up in the first decomposition step does not show a thermal stability for high temperatures in the TG experiments. The difference between the samples with and without red phosphorus arises only from the increased temperature range in which the residue of the first decomposition characterizes the material. We assume that in the case of red phosphorus-containing samples the residue of the first decomposition step could act as barrier for heat and volatile products. Consequently, the pyrolysis temperature is decreased during the combustion compared to that of samples without red phosphorus. It seems that the effective temperature in the pyrolysis zone moving through the sample with red phosphorus is decreased for low external heat fluxes, such that an increasing amount of residue from the first decomposition step remains as a stable residue. For high heat fluxes the effective temperature in the samples is still high enough to degrade the material almost completely. To illustrate this interpretation we made the following estimation.

During the combustion of a typical polymer the pyrolysis takes place at the surface. The surface temperature of the sample for a cone calorimeter experiment increases almost linearly until the ignition temperature is reached. After ignition, the pyrolysis at the surface occurs approximately at a constant temperature during the combustion. Obviously, this description does not perfectly fit our samples, given that the pyrolysis does not take place at the surface after the char formed covers the sample. However, we compared the residues obtained after the combustion in the cone calorimeter with the residues for isothermal TG experiments. The latter residues were calculated based on the activation energies for the decomposition we discussed before. The corresponding time for the residues after the cone calorimeter experiment was corrected with the ignition time. Table III shows the results of this comparison in terms of an effective decomposition temperature during the CC experiment for A3EG5 and A3X3G5. The heat flux determining the temperature consists of the external heat flux and the thermal feedback from the flame. The

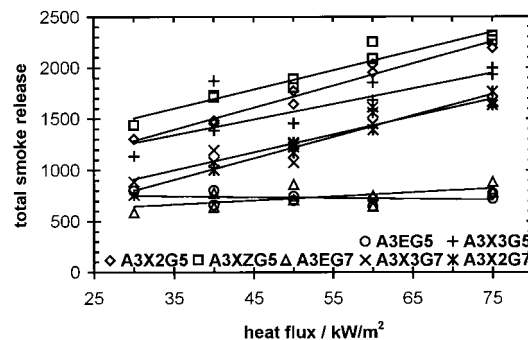
Table III Estimated Effective Pyrolysis Temperature

		A3EG5				
Heat flux in kW/m ²		30	40	50	60	75
<i>T</i> (pyrolysis) in K		693	706	711	723	718
		A3X2G5				
Heat flux in kW/m ²		30	40	50	60	75
<i>T</i> (pyrolysis) in K		643	667	684	699	708

char-forming systems are characterized by effective pyrolysis temperatures lower than those for the samples without red phosphorus. The non-char-forming system shows an increase in temperature about 30 K for external heat fluxes between 30 and 75 kW/m², whereas the char-forming system is characterized by a larger increase of 65 K in the same range of external heat fluxes. Even though the exact values cannot be directly used, taking into account the rough character of the approximate model applied, the qualitative result provides meaningful evidence and illustrates our interpretation.

Combustion Behavior: Fire Hazards

As the main fire hazard, production of smoke and CO was considered for the investigated system. The CO production per mass loss and the total smoke production are almost constant for the materials without red phosphorus. The CO production per mass loss is increased for the red phosphorus, for instance, from 0.0142 to 0.1344 kg/kg in terms of the 6-min average after ignition. The mass loss is not decreased by the same factor and the difference in total mass loss decreases for higher external heat fluxes. Consequently, the absolute CO production is increased. Similar behavior is found for the smoke production. The smoke production per mass loss as well as the total smoke production is increased for samples containing red phosphorus (Fig. 12). Both results indicate a less complete oxidation in the flame that, as discussed earlier, could not be confirmed by a change in the relationship between heat release and mass loss. The characterization of the fire hazard completes the investigation on the fire-retardant systems examined in this study, even though further investigations are required to provide a more detailed understanding.

**Figure 12** Total smoke release versus the external heat flux.

CONCLUSIONS

Red phosphorus acts as a flame retardant in the solid state mainly by influencing the kinetics of the decomposition processes of fiber-reinforced PA66. The main products released as volatiles were unambiguously identified by using both TG-MS and TG-FTIR. The samples were characterized by complex multistep decomposition under nitrogen with two major processes. The main process is connected to the release of NH₃, CO₂, H₂O, and cyclopentanone, whereas the subsequent decomposition is characterized by hydrocarbons and amines. The same products were identified for both samples without and with red phosphorus, whereas the temperature region of the decomposition is broadened for red phosphorus-containing materials. This broadening results in the separation of the two main decomposition steps, so that the system is changed from a non-char-forming to a char-forming material with respect to the main decomposition. The activation energies of the decompositions depend on the conversion. A moderate increase of the activation energies from about 120 kJ/mol is found up to a conversion of 60%. Beyond this conversion level a strong increase of the activation energies occurs to values > 220 kJ/mol. Both materials without and with red phosphorus show qualitatively similar characteristics, although the activation energies for high conversions are clearly decreased by red phosphorus.

The fire retardancy observed could be attributable to the char-forming behavior, which works in two different ways. The produced char acts like a barrier layer for the mass and the heat transfer, resulting in a decrease of the heat release rate. Furthermore, we assume that the decrease of the volatile products release leads to a decrease of

heat production in the flame zone, providing an enhancing feedback effect. Second, an increase of the remaining residue results in a decrease of the total amount of released combustible volatiles and therefore to a decrease in the total heat release. Most notable is that the first effect expands with increasing external heat flux, whereas the second effect vanishes almost completely. This could be explained by the fact that the obtained char does not show a thermal stability for higher temperatures as it is shown with TG experiments. The barrier mechanism decreasing the mass and heat release rate is also active for this char, which is stable for only a limited time interval if the char is produced continuously in the pyrolysis zone during burning. The second mechanism is based on the formation of char, which increases the thermally stable residue. It is concluded that only for smaller external heat fluxes is the effective pyrolysis temperature decreased, such that the char formed contributes to the residue.

The authors thank BASF AG (Ludwigshafen, Germany), especially Dr. J. Engelmann and Dr. F. Gruber (both Polymer Laboratory) for their support, which enabled us to carry out this work.

REFERENCES

- Piechota, H. *J Cell Plast* 1965, 1, 186.
- Peters, E. N. *Flame Retard Polym Mater* 1979, 5, 113.
- Davis, J.; Huggard, M. *J Vinyl Additive Technol* 1996, 2, 69.
- Levchik, S. V.; Weil, E. D.; Lewin, M. *Polym Int* 1999, 48, 532.
- Levchik, G. F.; Levchik, S. V.; Camino, G.; Weil, E. D. in *Fire Retardancy of Polymers: The Use of Intumescence*; Le Bras, M.; Camino, G.; Bourbigot, S.; Delobel, R., Eds.; The Royal Society of Chemistry: Cambridge, UK, 1998; pp 304–315.
- Steppan, D. D.; Doherty, M. F.; Malone, M. F. *J Appl Polym Sci* 1991, 42, 1009.
- Kunze, R.; Neubert, D.; Brademann-Jock, K. *J Therm Anal* 1998, 53, 27.
- Babrauskas, V.; Twilley, W. H.; Parker, W. J. *Fire Mater* 1993, 17, 51.
- Levchik, S. V.; Costa, L.; Camino, G. *Polym Degrad Stab* 1994, 43, 43.
- Pearce, E. M.; Shalaby, S. W.; Barker, R. H. in *Flame Retardant Polymeric Materials*; Lewin, M.; Atlas, S. M.; Pearce, E. M., Eds.; Plenum Press: New York, 1975; Vol. 1, p 239.
- Dussel, H.-J.; Rosen, H.; Hummel, D. O. *Makromol Chem* 1976, 177, 2343.
- Ohtani, H.; Nagaya, I.; Sugimura, Y.; Tsuge, S. *J. Anal Appl Pyrol* 1982, 4, 117.
- Hornsby, P. R.; Wang, J.; Rotheron, R.; Jackson, G.; Wilkinson, G.; Cossick, K. *Polym Degrad Stab* 1996, 51, 235.
- Pleebes, L. H., Jr.; Huffmann, J. *Polym Sci A-1* 1971, 9, 1807.
- Vyazovkin, S.; Linert, W. *Anal Chim Acta* 1994, 295, 101.
- Vyazovkin, S.; Goryachko, V. *Thermochim Acta* 1992, 194, 221.
- Vyazovkin, S. V.; Lesnikovich, A. I. *Thermochim Acta* 1992, 203, 177.
- Levchik, S. V.; Costa, L.; Camino, G. *Polym Degrad Stab* 1992, 36, 31.
- Rhodes, B. T. Burning rate and flame heat flux for PMMA in the cone calorimeter; NIST-GCR-95-664, 1994.
- Hopkins, D., Jr. Predicting the ignition time and burning rate of thermoplastics in the cone calorimeter; NIST-GCR-95-677, 1995.